ISBN: 978-3-95450-214-1 ISSN: 2673-5490 doi:10.18429/JACoW-IPAC2021-THPAB176

STUDIES ON BEAM COLLIMATION SYSTEM FOR THE ESSnuSB ACCUMULATOR*

Y. Zou†, M. Olvegård, Uppsala University, Uppsala, Sweden

Abstract

The ESSnuSB, a neutrino facility based on the European Spallation Source, aims at measuring, with precision, the charge-parity violating lepton phase at the 2nd oscillation maximum. The ESS linac will be upgraded to provide an additional 5 MW beam for the neutrino facility to produce an unprecedented high-intensity neutrino beam. An accumulator ring is employed to compress the 3 ms long pulse from the linac to four 1.2 μs short pulses in order to satisfy the target requirements and improve the physics performance. In the operation of a high-intensity proton accumulator, the most important issue is to minimize the uncontrolled beam loss in order to reduce the component activation and to make hands-on maintenance possible. For this purpose, a two-stage collimation system is designed, which consists of a thin scraper to scatter halo particles and secondary collimators to absorb those scattered particles. Phase advances between scraper and secondary collimators, together with the material, thickness of collimators, have been detailed studied and numerical simulations have been performed to evaluate the performance of the collimation system. This paper presents the first design of the collimation system.

INTRODUCTION

The European Spallation Source (ESS) [1], presently under construction in Lund, Sweden, will be the world's most powerful neutron source. Its superconducting linac accelerates proton pulses to 2 GeV, at a repetition rate of 14 Hz and a duty cycle of 4%. The RF cavities in the linac have the ability to accept a duty cycle of up to 10%, which leaves room for a neutrino facility by doubling the repetition rate. To this end, the ESS linac can, with moderate modifications, be used for the production of a very intense neutrino beam, the ESS neutrino Super Beam (ESSnuSB) [2-4].

In order to improve the performance of the neutrino experiment, the ESSnuSB will raise the ESS beam energy from 2.0 GeV to 2.5 GeV. H^- will be accelerated in the linac, interleaved with proton pulses for neutron facility, and injected into the accumulator ring with the charge-exchange injection method. To mitigate the space-charge issue in the accumulator, the linac pulse will be accumulated in four equal batches and the beam intensity for each batch will be reduced to 2.23×10^{14}. Figure 1 shows the sketch layout of the ESSnuSB accumulator with transfer lines on the ESS site.

The current accumulator lattice has a 384 m circumference with four super periods in order to suppress structural resonances. Each of the four arcs contains four FODO cells and has a horizontal phase advance of 2 π for closed dispersion. The four straight sections will be used for beam injection, collimation, extraction, and RF cavities, respectively. Studies of the beam injection, extraction, and RF cavities for this accumulator can be seen in [5-8]. Table 1 shows the main parameters.

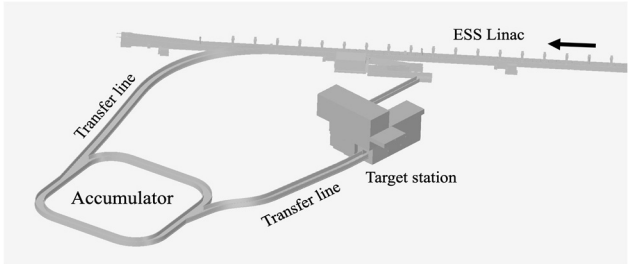

Figure 1: Sketch layout of the ESSnuSB accumulator with transfer lines on the ESS site [9].

Table 1: The Main Parameters of the Accumulator

Parameter	Value
Circumference (m)	384
Length of Straight / Arc (m)	56 / 40
Max. Beta Hor. / Ver. (m)	28.4 / 35.0
Tune Hor. / Ver.	8.24 / 8.31
Natural chromaticity Hor. / Ver.	-11.1 / -12.5
Betatron acceptance (π mm mrad)	200
Momentum acceptance	±1%

BEAM COLLIMATION SYSTEM

The beam collimation system is employed to clean the beam from halo particles in the ring to reduce the radioactivation damage and make hands-on maintenance available. Given that 5 MW of average beam power would be stored in the ring, a collimation system with a collimation efficiency of higher than 90% is required, according to the experience from the similar accelerators in the world, e.g. the SNS [10] and J-PARC [11]. A two-stage collimation system is designed for the ESSnuSB accumulator.

Two-Stage Collimation System

Two-stage collimation system for the ESSnuSB accumulator includes a thin scraper, which is the primary collimator, to increase the scattering angle of the beam halo particles, followed by four thick collimators, two in horizontal plane and two in vertical plane, the secondary collimators, to absorb the scattered beam halo particles. The main advantage compared to the traditional single-stage collimation system is that it can increase the impact parameter of the particles at the front of the secondary collimators which

* Work supported by European Union Horizon 2020
† ye.zou@physics.uu.se

ISBN: 978-3-95450-214-1 ISSN: 2673-5490 doi:10.18429/JACoW-IPAC2021-THPAB176

can dramatically improve the collimation efficiency, which is defined as the ratio of particles lost on the collimators to the total particle loss in the ring.

The straight section after the injection will accommodate the collimation system. To leave enough room for downstream placement of secondary collimators, the primary collimator is located before the center of the straight section, where $\beta_x = \beta_y$. Figure 2 shows the lattice function for one lattice super-period and the location of the primary collimator.

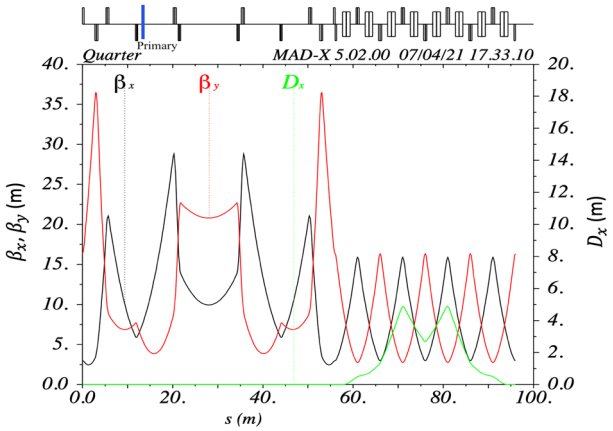

Figure 2: Lattice function for one lattice super-period. Blue line at the top marks the primary collimator location.

The optimal phase advance between the primary and the secondary collimator, for maximum interception efficiency, can be calculated as [12]:

$$\mu_{\mathrm{opt}} = \arccos(n_{\mathrm{prim}}/n_{\mathrm{sec}}), \quad (1)$$

where n_{prim} and n_{sec} are half apertures of primary and secondary collimators normalized to RMS beam size. For the ESSnuSB accumulator, considering the acceptance of primary and secondary collimators as 70 π mm mrad and 120 π mm mrad, respectively, we can get n_{prim}=2.35, n_{sec}=3.07, and the optimal phase advance from Eq. (1) approximately equals to 40º. So, the secondary collimators are ideally located at 40º and its complementary location 140º. Considering the real lattice situation, the phase advances of the secondary collimators are shown in Table 2.

Table 2: Collimator Information

Name	Type	Phase advance Hor. / Ver.
Prim	Horizontal/Vertical	0º / 0º
Sec_V1	Vertical	20º / 38º
Sec_H1	Horizontal	40º / 96º
Sec_V2	Vertical	90º / 121º
Sec_H2	Horizontal	130º / 154º

Material and Thickness for Primary Collimator

The material choice of the primary collimator normally follows two rules: 1) small energy loss and 2) large multi-Coulomb scattering angle. Figure 3 shows the comparison of RMS scattering angle together with energy loss for 2.5 GeV of proton beams interaction with a variety of materials. After also considering the availability, heat tolerance, melting point, and thermal conductivity, tantalum, tungsten, and platinum are good choices for the primary collimator.

The thickness choice for primary collimator is also a balance between scattering angle and energy loss to the proton beam. A thick scraper also increases the probability of large angle scattering, which may cause particle loss downstream before reaching the first secondary collimator. Figure 4 shows an example of the RMS scattering angle and energy loss for a 2.5 GeV proton beam interacting with tantalum of different thicknesses. If we choose the RMS scattering angle larger than e.g. 4 mrad and the energy loss less than e.g. 1%, the thickness of 6-20 g/cm^2 is expected to be a good choice.

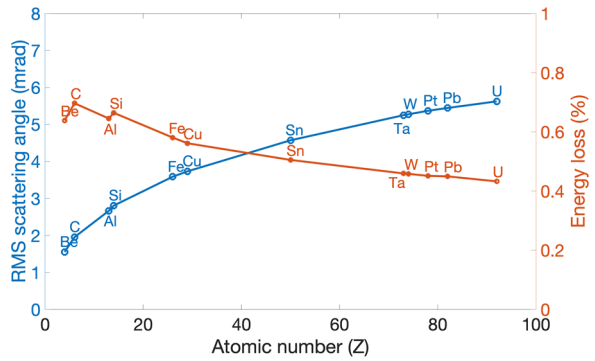

Figure 3: The RMS scattering angle and energy loss for 2.5 GeV of proton interaction with different materials with the thickness of 10 g/cm^2.

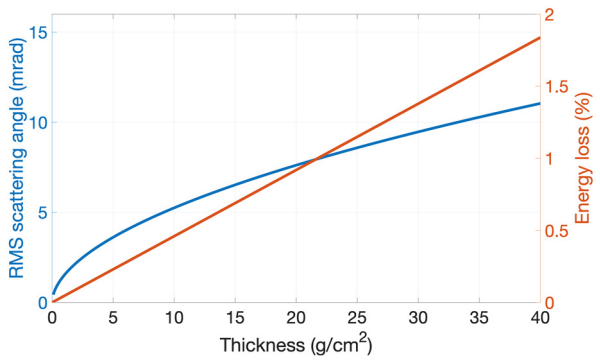

Figure 4: The RMS scattering angle and energy loss for 2.5 GeV protons interacting with different thickness of tantalum.

Numerical Simulations

Multi-particle simulations have been performed with the PyORBIT code [13] to evaluate the performance of the collimation system.

Since the collimation system only affects the beam halo particles, to simplify the simulation process, initial particles will have a larger amplitude than the primary collimator aperture, starting just at the front of the primary collimator, which means all particles will hit the primary collimator first. Initial particle distribution is in "L" type in real

ISBN: 978-3-95450-214-1 ISSN: 2673-5490 doi:10.18429/JACoW-IPAC2021-THPAB176

space with a typical width of 10 μm and a uniform distribution, which matches the shape of the primary collimator. Space charge effects are not included in the simulation.

Tantalum with 10 g/cm^2 of thickness is chosen for the primary collimator and tungsten with 1.5 m of length for the secondary collimators. Locations of the secondary collimators are shown in Table 2. In order to compare the particle loss rate for different collimator types, three types of secondary collimator combinations are studied: 1) all collimators in two-sided type, 2) first collimator in rectangular type and others in two-sided type, and 3) all collimators in rectangular type.

Figure 5 shows the particle loss rate in the collimation section with different types of configurations. For type 1, the major particle loss in the collimation section other than in the collimators appears just after the first secondary collimator. Changing the first secondary collimator into a rectangular type (type 2) reduces the beam loss after the first secondary collimator from around 7% to less than 1%. For type 3, beam loss after other secondary collimators can also be reduced. Figure 6 shows the beam loss map of the whole ring with the configuration of type 3. The collimation efficiency can reach 97%, which is 2% higher than type 2 and 12% higher than type 1.

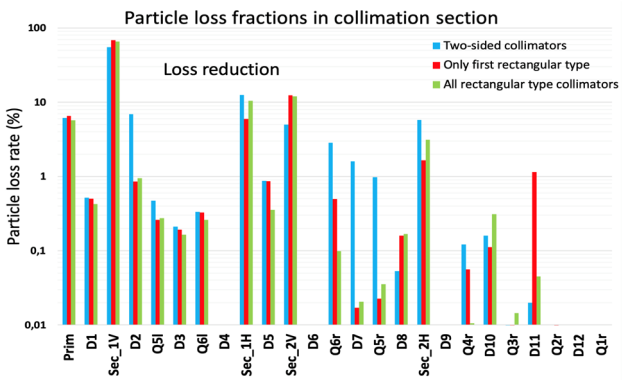

Figure 5: Particle loss rate in collimation section with different collimator types.

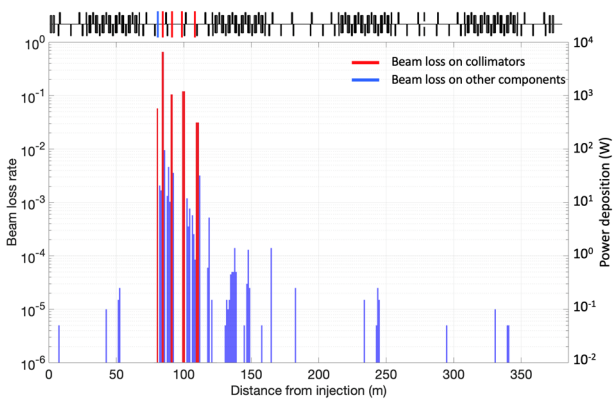

Figure 6: Beam loss map of the ring with the configuration of type 3.

Studies of the relationship between collimation efficiency, ring acceptance, and primary collimator thickness are also performed. Figure 7 shows the relationship between collimation efficiency and the ring acceptance. The collimation efficiency increases with the ring acceptance and comes to a quasi-flat top when the acceptance comes to about 200 π mm mrad. Figure 8 shows collimation efficiency and the power loss before reaching the secondary collimators with the thickness of the primary collimator. The collimation efficiency rises to a quasi-flat top when the thickness of primary collimation comes to 6 g/cm^2 while the power loss continues increasing due to the large angle scattering of the primary collimator.

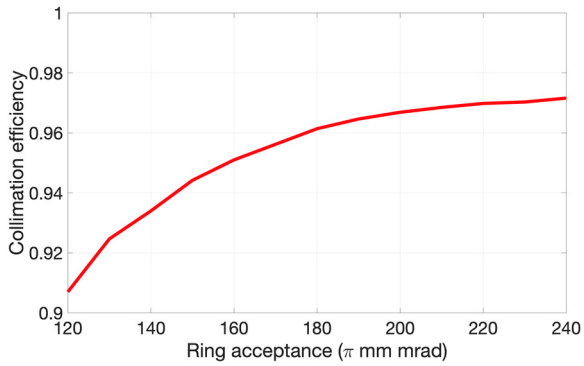

Figure 7: Relationship between the collimation efficiency and the ring acceptance.

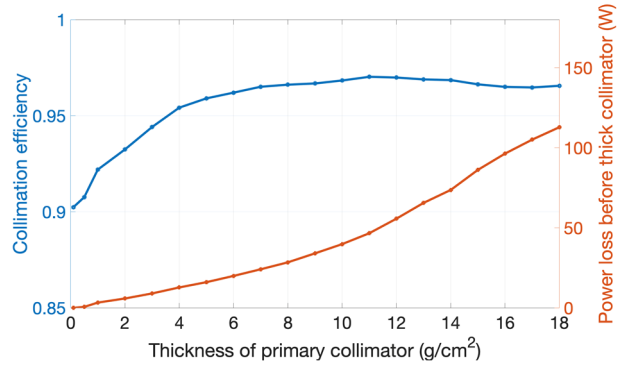

Figure 8: The collimation efficiency and the power loss before reaching secondary collimators as a function of the thickness of the primary collimator.

CONCLUSION

The basic collimation system for the ESSnuSB accumulator has been designed and numerical simulations have been performed to evaluate its performance. The collimation efficiency can reach 97%. Further optimization work is ongoing.

ACKNOWLEDGMENTS

This project is funded by the European Union Horizon 2020 research and innovation programme under grant agreement No. 777419.

ISBN: 978-3-95450-214-1 ISSN: 2673-5490 doi:10.18429/JACoW-IPAC2021-THPAB176

REFERENCES

[1] S. Peggs, "ESS Technical Design Report", ESS, Lund, Sweden, Rep. ESS-DOC-274, Apr. 2013.

[2] E. Wildner *et al.*, "The Opportunity Offered by the ESSnuSB Project to Exploit the Larger Leptonic CP Violation Signal at the Second Oscillation Maximum and the Requirements of This Project on the ESS Accelerator Complex", *Advances in High Energy Physics*, vol. 2016, no. 7, pp. 1-16, Oct. 2016. doi:10.1155/2016/8640493

[3] E. Baussan *et al*., "Neutrino super beam based on a superconducting proton linac", *Phys. Rev. Accel. Beams*, vol. 17, no. 3, p. 031001, Mar. 2014, doi:10.1103/PhysRevSTAB.17.031001

[4] M. Olvegaard *et al.*, "Overview of the ESSnuSB Accumulator Ring", in *Proc. 57th ICFA Advanced Beam Dynamics Workhop on High-Intensity and High-Brightness Hadron Beams (HB'16)*, Malmö, Sweden, Jul. 2016, pp. 105-109. doi:10.18429/JACoW-HB2016-MOPR021

[5] Y. Zou *et al.*, "Status of the ESSnuSB Accumulator Design", in *Proc. 10th Int. Particle Accelerator Conf. (IPAC'19)*, Melbourne, Australia, May 2019, pp. 666-668. doi:10.18429/JACoW-IPAC2019-MOPRB046

[6] Y. Zou, "The Accumulator Ring for the ESSnuSB Project - a progress report", in *Proc. 21st Int. Workshop on Neutrinos from Accelerators (NuFact'19)*, Daegu, Korea, Aug. 2019, p. 061. doi:10.22323/1.369.0061

[7] Y. Zou, "Challenges and Status of the ESSnuSB Accumulator Design", in *Proc. 20th Int. Workshop on Neutrinos from Accelerators (NuFact'18)*, Virginia, USA, Aug. 2018, p. 117. doi:10.22323/1.341.0117

[8] A. Alekou *et al*., "Design of a Fast Single-turn Extraction for the ESSnuSB Accumulator", CERN, Geneva, Switzerland, Rep. CERN-ACC-2020-0027, Aug. 2020

[9] N. Gazis, "Near Detector location & layout at the ESS site", presented at *ESSnuSB WP5+6 meeting*, Zagreb, Croatia, Oct. 2019, unpublished.

[10] D. Jeon *et al*., "In-Beam SNS Ring Collimation Optimisation", in *Proc. the 1999 Particle Accelerator Conf*., New York, USA, Mar.-Apr. 1999, pp. 3303-3305. doi:10.1109/PAC.1999.792284

[11] K. Yamamoto, "Efficiency simulation for the beam collimation system of the Japan Proton Accelerator Research Complex rapid-cycling synchrotron", *Phys. Rev. Spec. Top. Accel. Beams*, vol. 11, no. 12, p. 123501, Dec. 2008. doi:10.1103/PhysRevSTAB.11.123501

[12] J. B. Jeanneret, "Optics of a two-stage collimation system", *Phys. Rev. Spec. Top. Accel. Beams*, vol. 1, no. 8, p. 081001, Dec. 1998. doi:10.1103/PhysRevSTAB.1.081001

[13] A. Shishlo, S. Cousineau, J. Holmes, and T. Gorlov, "The Particle Accelerator Simulation Code PyORBIT," *Procedia Computer Science*, vol. 51, pp. 1272–1281, 2015. doi:10.1016/j.procs.2015.05.312